Real-Time Array Feed Compensation System Demonstration at JPL

V. Vilnrotter, D. Fort and B. Iijima

Jet Propulsion Laboratory, California Institute of Technology, Pasadena, CA

Abstract

A real-time array feed compensation system has been constructed, and is currently undergoing tests at JPL. This sytem was designed to operate at h-band (33.7 GHz) carrier frequencies, where mechanical distortions begin to seriously degrade the performance of large DSN antennas. A compact cluster of seven 22 dBi horns in the focal-plane of a 34-meter beam-waveguide antenna sample the distorted fields, and optimum combining-weights are derived from correlation measurements on the downconverted baseband signals. The instrument used to carry out these measurements is a real-time correlator built primarily for VLBI applications, and hence can be used to observe broadband sources such as quasars and planets. In addition to providing combining information, the correlation coefficients are used to characterize the" atmosphere's contribution to the total system noise, and to derive pointing corrections which help to keep the antenna pointed on source.

I. Introduction

There is considerable interest in operating the Deep Space Network (DSN) at increasing higher frequencies for enhancing its telemetry and radio science capabilities [2,3]. Higher carrier frequencies yield greater antenna gains, as well as reduced sensitivity to plasma effects, and increased useful bandwidth. However, antenna surface errors induced by gravity or wind become more significant at high frequencies due to the shorter wavelengths, resulting in degraded performance. Some of these performance losses can be recovered, in principle, by a real-time compensation system employing a properly designed array of horns in the focal-plane.

A seven element Ka-band (33.7 GHz) focal-plane array feed compensation system has been constructed at JPL for the purpose of demonstrating recovery of signal-to-noise ratio (SNR) losses due to gravity and wind-induced deformations on large receiving antennas. Initially, concept demonstrations have taken place on a 34 meter beam-waveguide (BWG) antenna located at the Goldstone antenna facility of the Deep Space Network in California, but plans are to demonstrate the system on a 70 meter antenna as well in the near future. The feed array, along with the cryogenically cooled HEMT low-noise amplifiers and RF to IF downconverters, is located in the pedestal-room of the antenna; the VLBI video converters, real-time correlator and the digital combining system are located in the control room, some 300 meters away.

Antenna performance is often specified in terms of efficiency, which is defined as the ratio of output to incident signal powers. Loss in efficiency leads directly to comparable losses in SNR when observing radio sources or spacecraft. Elevation-dependent efficiency losses have been measured on several DSN antennas at IQ-band. The elevation dependence of the efficiency for two DSN antennas is shown in Fig. 1: the 34 meter antenna at DSS 13 loses 3 dB at zenith and over 2 dB below 20 degrees, while the 70 meter antenna 'at DSS 14 is virtually unusable above 75 or below 15 degrees.

A schematic diagram of the beam-waveguide antenna is shown in Fig. 2. The cassegrain focus, Fl, is transferred down the waveguide by means of parabolic and flat reflectors to a point eight meters above the pedestal-room floor. This second focal point, F2, corresponds to one of the foci of a rotatable ellipsoidal mirror: the feed array is located at the other focus, F3. By rotating the ellipsoid around the BWG axis, different receivers can be accessed.

A conceptual design of the surface compensation system is shown in Fig. 3. The received RF fields, consisting of both desired signal fields and unwanted background radiation, are concentrated onto an array of horns at the antenna's focal plane, here shown at the antenna's cassegrain focus. The received fields are converted to electrical signals, downconverted to baseband in-phase and quadrature samples, and processed digitally to extract the field parameters required for optimum combining. Finally, a weighted sum of samples from all of the channels is formed. If the weight estimates are accurate, the SNR of this combined channel exceeds that obtainable with any single receiving horn.

In addition to providing compensation for gravitational deformation, an array of horns in the focal-plane can also be used to extract pointing information. The basic idea is to use the approximate Fourier trnasform relation between the aperture and focal-plane field distributions: the normal to the phase-surface of the RF field impinging on the aperture can be estimated by measuring the magnitude and phase of the signal in each horn, and performing a two-dimensional inverse Fourier transform. An algorithm based on this approach has been developed, and is undergoing tests.

Independent confirmation of experimental results is always desirable, particularly when new concepts or techniques are analyzed. In the context of the Array Feed Compensation system demonstration, the correlator can also be used to predict combiner performance, in addition to obtaining real-time weight estimates from the one-bit quantized bit-stream. Direct comparison of the predicted SNR with the measured SNR of the combined signal can be used to verify system performance. In the following sections a simple expression will be derived. for the SNR of the combined signal when accurate combining weights are available, and its implementation with recorded data will be described.

II. Optimum combining weights for independent noise

Suppose the antenna points to a distant natural radio source (such as a planet or a quasar) which generates a broadband thermal signal, and that an independent noise waveform is added to each channel of the array. The received RF signal in the k-th channel may then be represented by

$$r_k(t) = s_k(t) + n_k(t) \quad k = 1,2,\ldots,K \tag{1a}$$

with source signal and background noise components

$$s_k(t) = \sqrt{2}S_k\left[a_c(t)\cos(\omega t + \theta_k) + a_s(t)\sin(\omega t + \theta_k)\right] \tag{1b}$$

$$n_k(t) = \sqrt{2}\left[n_{ck}(t)\cos(\omega t) + n_{sk}(t)\sin(\omega t)\right] \tag{1c}$$

where $a_c(t)$ and $a_s(t)$ are uncorrelated random processes representing the source signal, as are $n_{ck}(t)$ and $n_{sk}(t)$ which represent the background noise. The bandwidth of these random processes are assumed to be narrow compared to the carrier frequency ω: however, when downconverted to baseband, these processes are considered to be "broadband" signals. Since the source signals in the various channels differ from each other only in amplitude and phase (hence $a_c(t)$ and $a_s(t)$ are independent of k), the time-varying envelopes being identical, the random processes $s_k(t)$ are correlated. The background noise processes will be assumed uncorrelated in the analysis, as these consist of noise generated within the receivers plus background radiation arriving from different directions in space. (Actually, correlation coefficients on the order of 0.01 are typical between the feeds, probably due to near-field atmospheric noise: this issue is currently being investigated.) Following baseband downconversion and sampling, the in-phase and quadrature samples may be represented "by the complex process

$$\tilde{r}_k(i) = \tilde{s}_k(i) + \tilde{n}_k(i) \tag{2}$$

where $\tilde{s}_k(i) = \tilde{S}_k \tilde{a}(i)$, and $\tilde{S}_k = S_k e^{j\theta_k}$. Each component of the complex noise is independent with variance σ_k^2, but we shall assume that the real and imaginary components of $\tilde{a}(i)$ have variance 1/2, so as not to introduce additional scaling. Thus the signal-to-noise ratio (SNR) of $\tilde{r}_k(i)$ becomes $S_k^2/2\sigma_k^2$.

Let $\tilde{w}_k$ be a complex constant, and form the sum

$$\tilde{z}(i) = \sum_{k=1}^{K} \tilde{r}_k(i)\tilde{w}_k \tag{3}$$

where $\tilde{z}(i)$ is the weighted sum. With $\tilde{s}_C(i) = \sum_{k=1}^{K} \tilde{s}_k(i)\tilde{w}_k$ denoting the combined source signal component, the SNR of the combined sequence can be defined as

$$SNR_C = \left\langle \left| \tilde{s}_C(i) \right|^2 \right\rangle / \mathrm{var}\left\{ \sum_{k=1}^{K} \tilde{w}_k \tilde{n}_k(i) \right\} . \tag{4}$$

where the numerator is the expected value of the magnitude squared of the combined signal, and the denominator is just the variance of the weighted noise sum. As shown in references [2,3], the SNR of $\tilde{z}(i)$ is maximized when the complex weights $\{\tilde{w}_k\}$ are selected according to the formula

$$\tilde{w}_k = \tilde{S}_k^* / 2\sigma_k^2 . \tag{5}$$

(* denotes complex conjugate.) Substituting these complex combining weights into equation (4) yields

$$SNR_C = \frac{\left| \sum_{k=1}^{K} \tilde{S}_k \tilde{w}_k \right|^2}{\sum_{k=1}^{K} 2|\tilde{w}_k|^2 \sigma_k^2} = \sum_{k=1}^{K} S_k^2 / 2\sigma_k^2 \tag{6}$$

Thus, the SNR of the combined sequence is equal to the sum of the individual channel SNRS when optimum combining weights are used. The problem is that the optimum weights are not known *a priori*, hence must be estimated: in the presence of noise, these estimates are always subject to error.

The expression for optimum combining weights for a continuous wave source is very similar to the natural radio source case. The continuous wave signal in each of the feeds can be written as

$$s_k(t) = \sqrt{2} S_k \cos[\phi_{cw}(t) + \theta_k] \tag{7}$$

where $\phi_{cw}(t)$ is the RF signal phase. Following baseband downconversion and sampling, the in-phase and quadrature samples of the continuous wave signal may be represented by the complex process $\tilde{s}_k(i) = \tilde{S}_k e^{j\phi_{BB}}$ where $\tilde{S}_k = S_k e^{j\theta_k}$ and $\phi_{BB}(t)$ is the baseband signal phase. With these definitions, eqs. (2) through (6) apply in the continuous wave case, as well as the natural radio source case.

III. Array feed combining demonstration setup

A schematic of the array feed combining demonstration is shown in Figure 4. The signals from the 7 feeds are sent to the DSS 13 control room after downconversion to IF. (Typically, the IF frequency is in the 250-300 MHz range.) Each of the seven IFs is split into two signals, with one signal fed directly into the Mark III VLBI data-acquisition terminal (Mark III DAT), where it is downconverted to baseband. The second signal goes into a "trombone" before being downconverted to baseband. The trombone is a waveguide whose length can be adjusted so that at IF a narrowband signal passing through it is 90 degrees out of phase from the direct signal, giving rise to in-phase (I) and quadrature (Q) baseband signals for each of the 7 feeds. After downconversion, the baseband signals are sent to the Digital Signal Processor subsystem (DSP) for combining, and also to RTB2 where the combining weights are produced. The baseband signals are sampled at the Nyquist rate and single-bit quantized by the formatter of the Mark III DAT before being sent to RTB2. In the broadband signal case, the IF signal from the central feed is divided again and downconverted using a heterodyne frequency 10 kHz less than that used for the other 14 signals, and this frequency-offset signal is also sent to RTB2. (The reason for the 10 kHz offset is to ensure that both correlated signal amplitude and phase shift can be extracted from the correlation product. See Section IV.) Finally, RTB2 produces complex combining weights which are sent to the DSP where the 14 baseband signals are combined.

The real-time correlator is being used for two purposes: (1) to compute combining weights and pointing coefficients in real-time, and (2) to compute the SNR for the optimally combined array feed signal. The computation of the optimally combined SNR is performed off line. The computation of the combining weights is described in Section IV. The computation of the predicted optimally combined , SNR is described in Section V,

IV. Computing the combining weights

The computation of the combining weights will be discussed for two signal types: for a continuous wave signal, such as a spacecraft carrier wave, and for a broadband noise source.

RTB2 has two primary functions: (1) cross-correlating pairs of signal bitstreams, and (2) extracting tones (approximately sinusoidal signals) from individual signal bitstreams. In the cross-correlation process, pairs of signal bitstreams are multiplied together with a complex sinusoid and integrated. In the tone extraction process, individual signal bitstreams are multiplied by complex sinusoids and integrated. When weights are computed for a spacecraft carrier wave, tone extraction is used. When weights are computed for a broadband noise source, cross-correlation is used.

Computing combining weights for a continuous wave source

The phase and signal strengths in each of the 7 feeds can be obtained by correlating a model sinusoid both in-phase and quadrature with the signal from each of the 7 feeds, yielding the 7 complex (in-phase and quadrature) correlation sums ρ_k. The combining weights can be written as [1]

$$\tilde{w}_k = \frac{\rho_k^*}{|\rho_1|^2}\rho_1\sqrt{\frac{P_{n1}}{P_{nk}}} \qquad k= 1...7. \tag{8}$$

where P_{nk} *is* the noise power in the k-th channel. The overall phase and magnitude of the combining weights for the 7 feeds have been chosen so that feed number 1 has weight 1: this renders the weights dimensionless. In practice, the feeds have nearly identical noise power, so the last factor is typically ignored.

Computing combining weights for a broadband noise source

Computation of combining weights for an unresolved far-field broadband noise source is somewhat more complicated than for the continuous wave case. (Following is a condensed discussion of the combining weight computation. For a more complete discussion, see Ref. 1.) The signal from the central feed is correlated against the signals from the outer feeds in order to measure the relative phase

and source signal strength of each of the 7 feeds. So that both phase and signal amplitude can be measured, the version of the central feed signal heterodyned with a frequency offset of 10 kHz (as described in Section III) is correlated with each of the 7 feed signals: the product of the frequency-offset central feed signal with another feed signal will contain a 10 kHz sinusoid with amplitude proportional to the product of the signal strengths in the central feed and the other feed, and phase lag that is the relative phase between the two feeds. The 7 product signals are each correlated with a 10 kHz sinusoid both in-phase and quadrature yielding the 7 complex correlation sums ρ_k.

The correlation sums would directly give the relative signal strength and phase of the seven feeds except for two complications: (1) The background noise signals in the 7 feeds are correlated with each other (primarily due to common near-field atmospheric' thermal radiation) and thus contribute to the cross-correlation phase and amplitude. And (2) the correlation sums give information about the relative source signal strengths of the outer feeds but not of the outer feeds relative to the center feed. The first problem is resolved by subtracting correlation sums measured slightly off-source from the on-source correlation sums to give calibrated correlation sums ρ_k^{cal}. The second problem is resolved by measuring the central feed power on- and slightly off-source with a radiometer to get the SNR in the central feed.

Combining this with measurements of the central feed SNR and noise voltage measurements, one can compute the combining weights

$$\tilde{w}_k = \frac{\rho_k^{cal*}\rho_1}{\left|\rho_k^{cal}\rho_1\right|}\sqrt{\frac{P_{sk}/P_{nk}}{P_{s1}/P_{n1}}}\sqrt{\frac{P_{n1}}{P_{nk}}} \quad k = 1...7 \qquad \textbf{(9)}$$

where the SNR in outer feed *k is* computed from

$$\frac{P_{sk}}{P_{nk}} = \frac{\frac{P_{T1}}{P_{s1}}\left(\frac{\pi}{a}\right)^2\left(\left|\rho_k^{cal}\right|^2 - 2\sigma_c^2\right)}{1 - \frac{P_{T1}}{P_{s1}}\left(\frac{\pi}{a}\right)^2\left(\left|\rho_k^{cal}\right|^2 - 2\sigma_c^2\right)} \quad k = 2...7 \qquad \text{(lo)}$$

and where σ_ϵ^2 is a correlation sum error, negligible for a strong source, which is subtracted to remove a positive bias on the square magnitude ρ_k^{cal}. The overall magnitude and phase of the weights have been chosen to set $\tilde{w}_1$ equal to one. In practice, the feeds have nearly identical noise power, so that the last factor in eq. (9) is typically ignored,

V. Computation of optimal combined SNR

In eq. (6) it is shown that when the optimal weights are used, the SNR for the combined signal is the sum of the individual feed SNRS. By combining the direct radiometric measurement of the central feed SNR and the calibrated correlation sums ρ_k^{cal} one can compute the combined SNR expected for optimal weighting. Correlation sums were written to a post-correlation record file and processed off-line to produce this combined SNR.

The above computations have been carried out for a Jupiter boresight track on 1993 DOY 335 using the 34 m antenna at DSS-13. Plotted in Figure 5 are the central feed SNR and the optimal combined SNR (the sum of the central feed SNR plus the six ring feed SNRS as computed from eq. (10)). Also plotted are modifications to the SNR plot, eliminating the effects of elevation dependent noise power, and elevation dependent signal attenuation.

The elevation dependence in the noise power was obtained directly from the off-source power measurements. The elevation-dependent signal loss was estimated using station weather data (temperature, pressure and humidity) during the track, computing a zenith attenuation coefficient, and applying this value to an atmospheric loss model. Note that even at 42.5 degrees elevation the SNR of the combined channels (SNR_C) exceeds that of the central channel (SNR_1) by about 0.5 dB. (SNR_1 has been effectively "smoothed" on a greater time scale than the SNR_C curve.) The corrected combined signal-to-noise ratio SNR_C^{**} decreases by only 0,54 dB at low elevations while the corrected central channel loses about 1,12 dB of SNR at 9°, (This 34 m antenna is actually much better at Ka-band than the 70 m antennas used by the DSN, which suffer as much as 5 dB SNR loss over the same elevation

range [7]: hence, much greater SNR recovery can also be expected for a 70 m antenna.) Thus combining tends to provide uniform SNR over a range of elevations.

VI. Measured combining gain

The combining gain relative to the central channel has been measured, using combining weights estimated by RTB2 in real time. The digital combiner received the complex weights from RTB2, multiplied each sample by the appropriate combining weight for that (complex) channel, and summed the resulting samples. Power estimates were made for both the combined and central channels, and the results stored for comparison. The procedure for obtaining the combining gain consisted of 3 steps: first, the antenna was pointed slightly off-source (85 mdeg) and an estimate of the noise correlation vector obtained. Next, the antenna was pointed on-source and combining weights were estimated by subtracting the noise correlation estimate from the on-source coefficients. These corrected combining weights were used during data-gathering, which consisted of combined and central channel power measurements first on-source and then off. The reason for using the same combining weights both on and off-source is to keep the combined noise power constant, enabling a simple measurement of the combined signal power: otherwise, most of the change between on and off-source powers would be due to the weighted noise power rather than the signal.

The above data-gathering procedure was applied to a Venus track on March 4, 1993. Efficiency curves for the central and combined channels, corrected for atmospheric losses, are shown in Fig. 6 over an elevation range of 10 to 30 degrees. The combiner was sampling the complex baseband signals, limited to 200 kHz bandwidth, at ,635 kilo-samples per second. The effective integration time for the power measurements was about 0.25 seconds. Although the array feed was not optimally aligned at that time (so that the peak efficiency of the central channel was somewhat low), combining gains of 0.5 to 1.5 dB were measured. After accurate alignment and calibration of the entire front end is completed, these measurements will be repeated using various Ka-band radio sources to better characterize the performance of the combining system.

VII. Array Feed tracking algorithm

A focal-plane array can also be used to derive pointing error information from the received fields. The idea is to view the signal parameter estimates from each horn as samples of the focal-plane field. Then, making use of the inverse Fourier transform relation between the aperture and focal planes, these samples are used to obtain an approximation to the aperture-plane field distribution. The normal to the phase-plane near the center of the aperture is used to estimate the direction-of-arrival of the signal (a block diagram of the estimator structure is shown in Fig. 7a). In the absence of additive noise, this algorithm obtains accurate estimates of pointing-error over a six millidegree range, as shown in Fig. 7b. This performance curve was obtained using simulated focal-plane field distributions.

The digital tracking algorithm (DTA) was also tested in the field, using Jupiter as the source. The results of this experiment are shown in Fig. 8. The initial pointing error was reduced to less than one millidegree by means of a boresighting algorithm. Then, when exactly on-source, the DTA made estimates of the pointing error. These estimates were recorded, and displayed in Fig. 8 as clusters of circles near the origin. With 4 second integration, the RMS scatter is about 0.5 mdeg, which is perfectly adequate for an antenna with a 17 mdeg beamwidth. Similar performance was obtained when 4 mdeg errors were introduced into the antenna pointing. The slight rotation in these clusters is attributed to an error in the de-rotation algorithm, which attempts to remove the relative rotation between the antenna and array feed coordinate systems introduced by the beam waveguide.

VIII. Summary and conclusions

A technique has been described for estimating the optimum combining weights for the Array Feed Compensation system, both for received tones and broadband signals, observed in the presence of additive noise. In the derivation of the optimum combining weights, the noise components in the various channels were assumed to be independent even though correlations on the order of one percent

are routinely observed. These low-level correlations are believed to be primarily due to near-field atmospheric radiation. Although noise correlations of such small magnitude are not expected to affect the SNR of the weighted sum, their presence could introduce a large error into the weight estimates, , particularly when weak broadband sources are observed. Therefore, the noise correlations are measured slightly off-source, and subtracted from ρ_k before computing the combining weights. The combining weights thus obtained. can then be used for combining the signals from all of the feeds. Modifications to the combining weights to account for noise correlations are currently being examined.

The ability to compute channel SNRS based on the correlation coefficients is useful for estimating the SNR of the combined signal, which is simply the sum of the channel SNRS when accurate combining weights are available. (If the combining weights are in error, a loss in combined SNR will occur.) The above procedure has been carried out for a Jupiter track, from which we conclude that on the 34 m antenna at DSS-13 the combined channel loses only 0.54 dB in efficiency as the elevation varies from 43 degrees down to 9 degrees, after correction for elevation-dependent losses. This result confirms the ability of the Array Feed Combining system to improve the efficiency response of large DSN antennas. The technique will be applied to subsequent tracks, in order to accumulate data on combiner performance with a variety of sources under various conditions.

An additional advantage of the focal-plane array feed approach is that pointing information can also be extracted from the real-time signal parameter estimates, without the need for additional dedicated hardware. A simple algorithm has been installed at the station, and is currently being evaluated in an open-loop configuration. After these tests are complete, the error estimates will be fed back to the antenna controller, and closed-loop test will begin. An interesting question that remains to be addressed is the effect of surface distortions on the performance of the pointing algorithm at high or low elevations, and in the presence of wind,

References

[1] B. Iijima, D. Fort, and V. Vilnrott "Correlator Data Analysis for the Array Feed Compensation System," *Telecommunications and Data Acquisition Progress Report 42-117, vol. January-March 1994,* Jet Propulsion Laboratory, Pasadena, California, in press.

[2] V. A. Vilnrotter, E. R. Rodemich, and S. J. Dolinar, Jr., "Real-Time Combining of Residual Carrier Array Signals Using ML Weight Estimates," *IEEE Transactions on Communications, vol. 40,* no. 3, pp. 604-615, March 1992.

[3] V. A. Vilnrotter and E. R. Rodemich, "A Digital Combining-Weight Estimation Algorithm for Broadband Sources With the Array Feed Compensation System," *Telecommunications and Data Acquisition Progress Report 42-116, vol. October-December 1993,* Jet Propulsion Laboratory, Pasadena, California, pp. X-X, February 15, 1994.

[4] C. Edwards, D. Rogstad, D. Fort, L. White, and B. Iijima, "The Goldstone Real-Time Connected Element Interferometer," *TDA Progress Report 42-110, vol. April-June 1992,* Jet Propulsion Laboratory, Pasadena, California, pp. 52-62, August 15, 1992.

[5] J. B. Thomas, "The Tone Generator and Phase Calibration in VLBI Measurements," *DSN Progress Report 42-44, January and February 1978,* April 15, 1978, pp. 63-74.

[6] J. B. Thomas, "Interferometry Theory for the Block II Processor," JPL Publication 87-29, Jet Propulsion Laboratory, Pasadena, California, October, 1987.

[7] M. Gatti, et al, "32-GHz Performance of the DSS-14 70-Meter Antenna: 1989 Configuration," *TDA Progress Report 42-99,* Jet Propulsion Laboratory, Pasadena, California, pp. 206-219, November 15, 1989.

[8] S. T. Lowe, "Theory of Post-Block II VLBI Observable Extraction," JPL Publication 92-7, Jet Propulsion Laboratory, Pasadena, California, July 15, 1992.

DSS 14

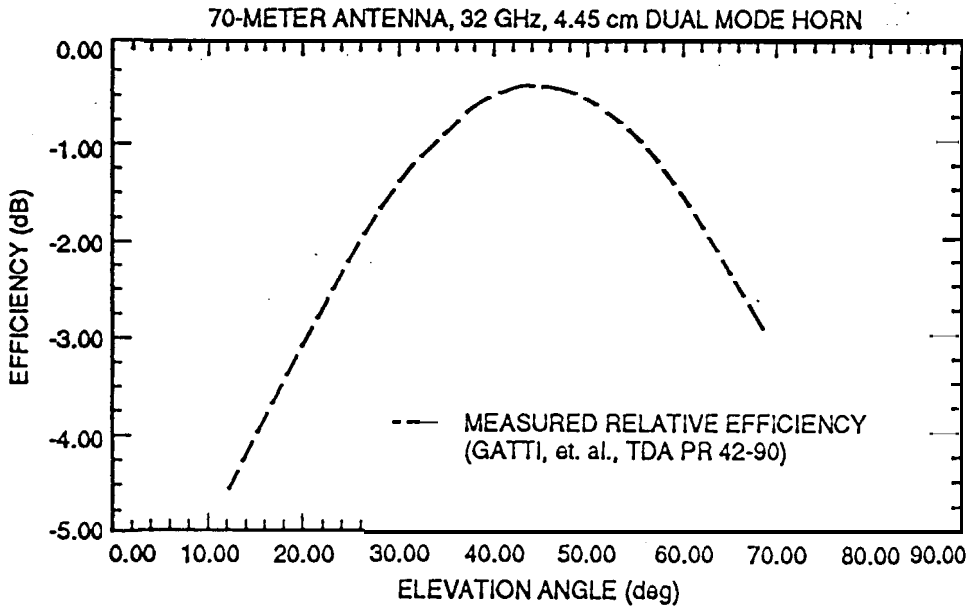

DSS 13 X- & K_a-BAND EFFICIENCY AT F1

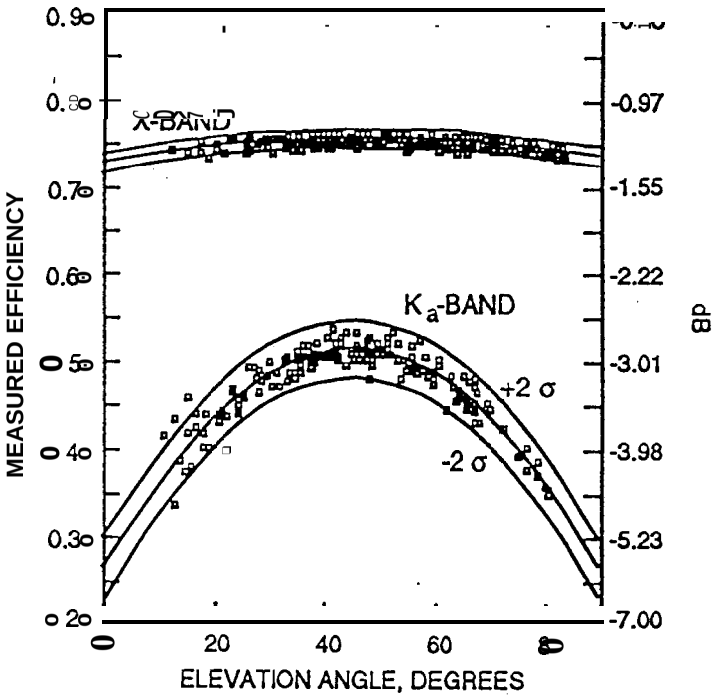

Figure 1. Efficiency of DSN Antennas a K_a-band

6485-36447u

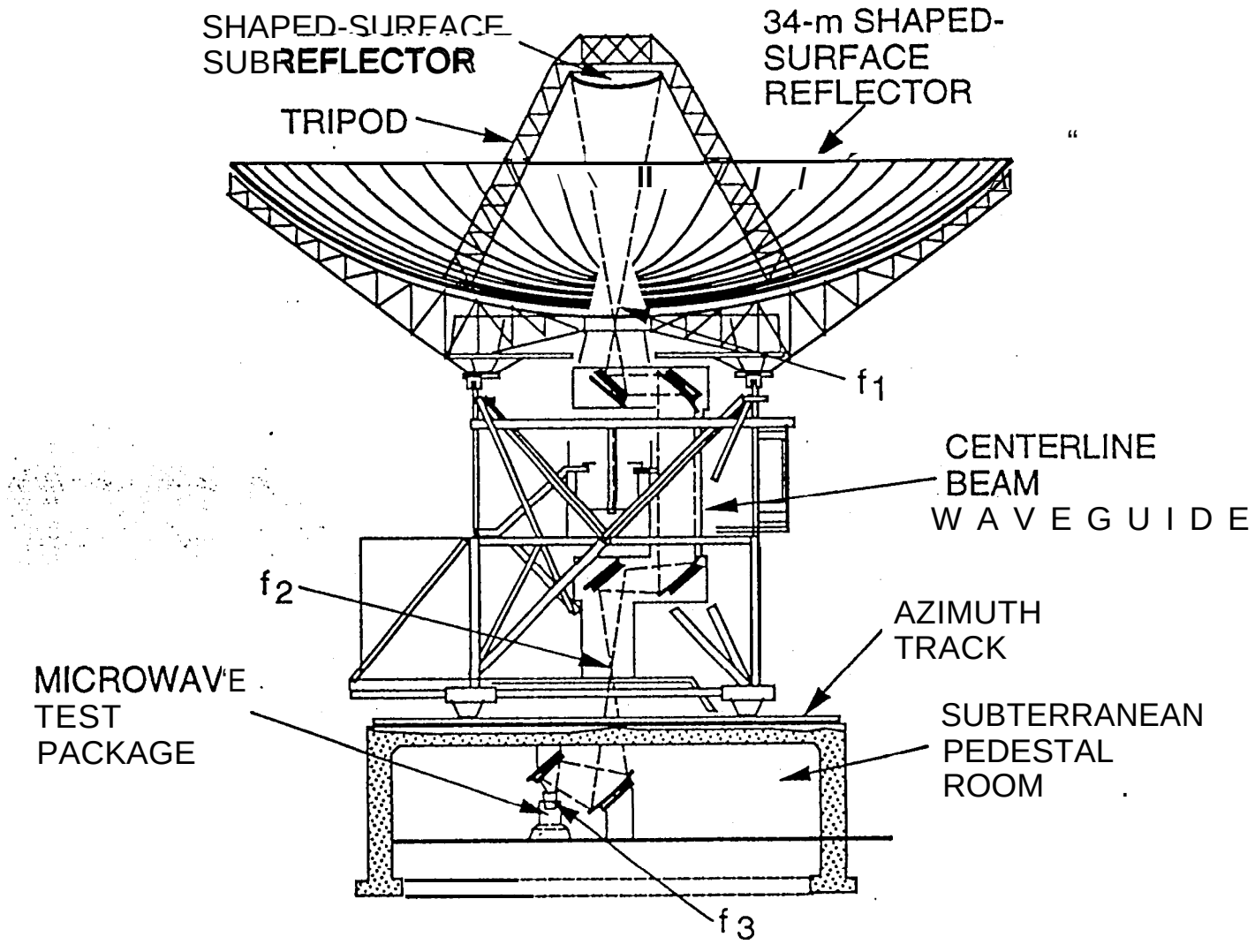

Figure 2. 34-Meter Beam Waveguide Antenna

6485-36448u

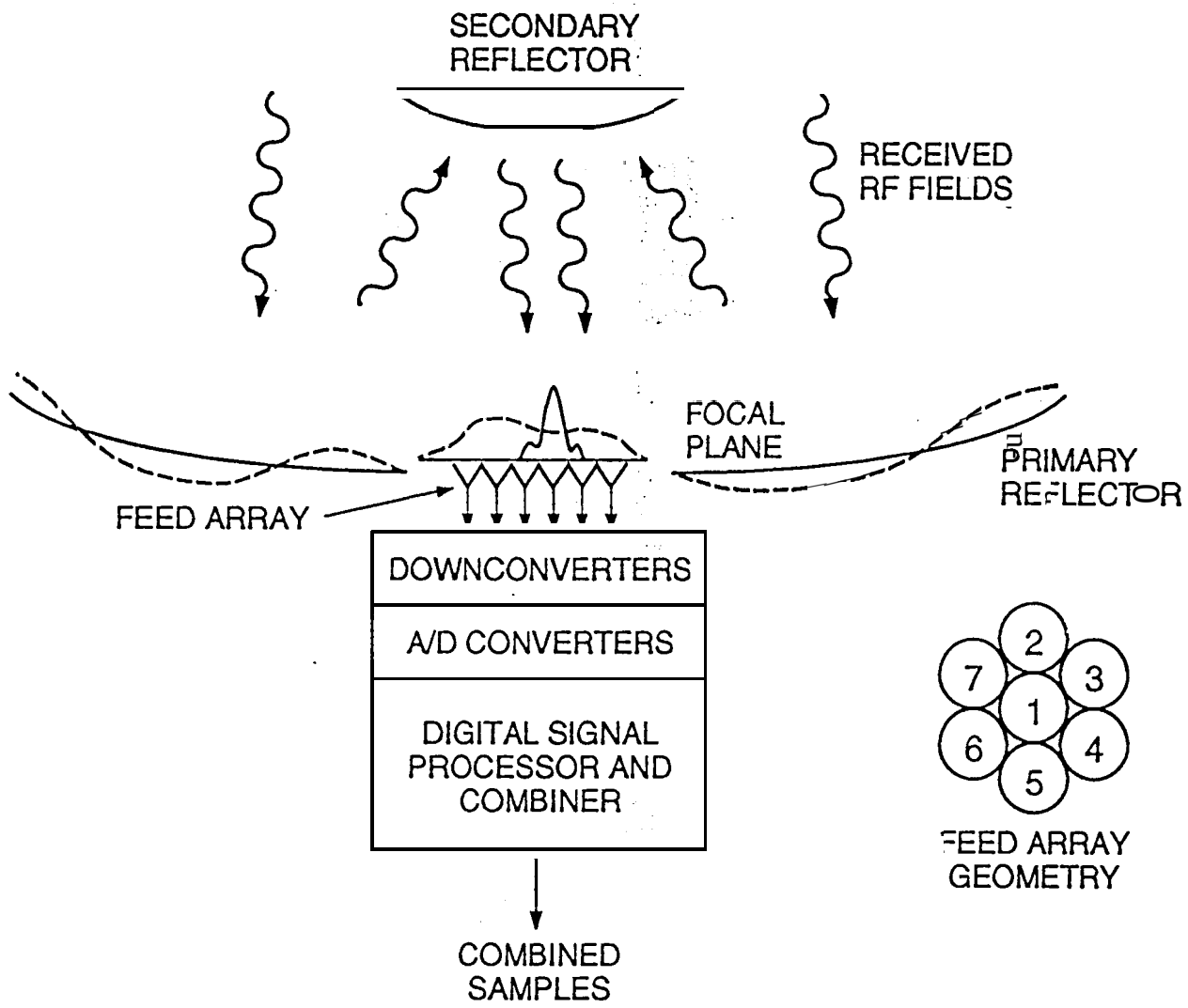

Figure 3. Real-Time Antenna-Compensation System Conceptual Design

6485-36449u

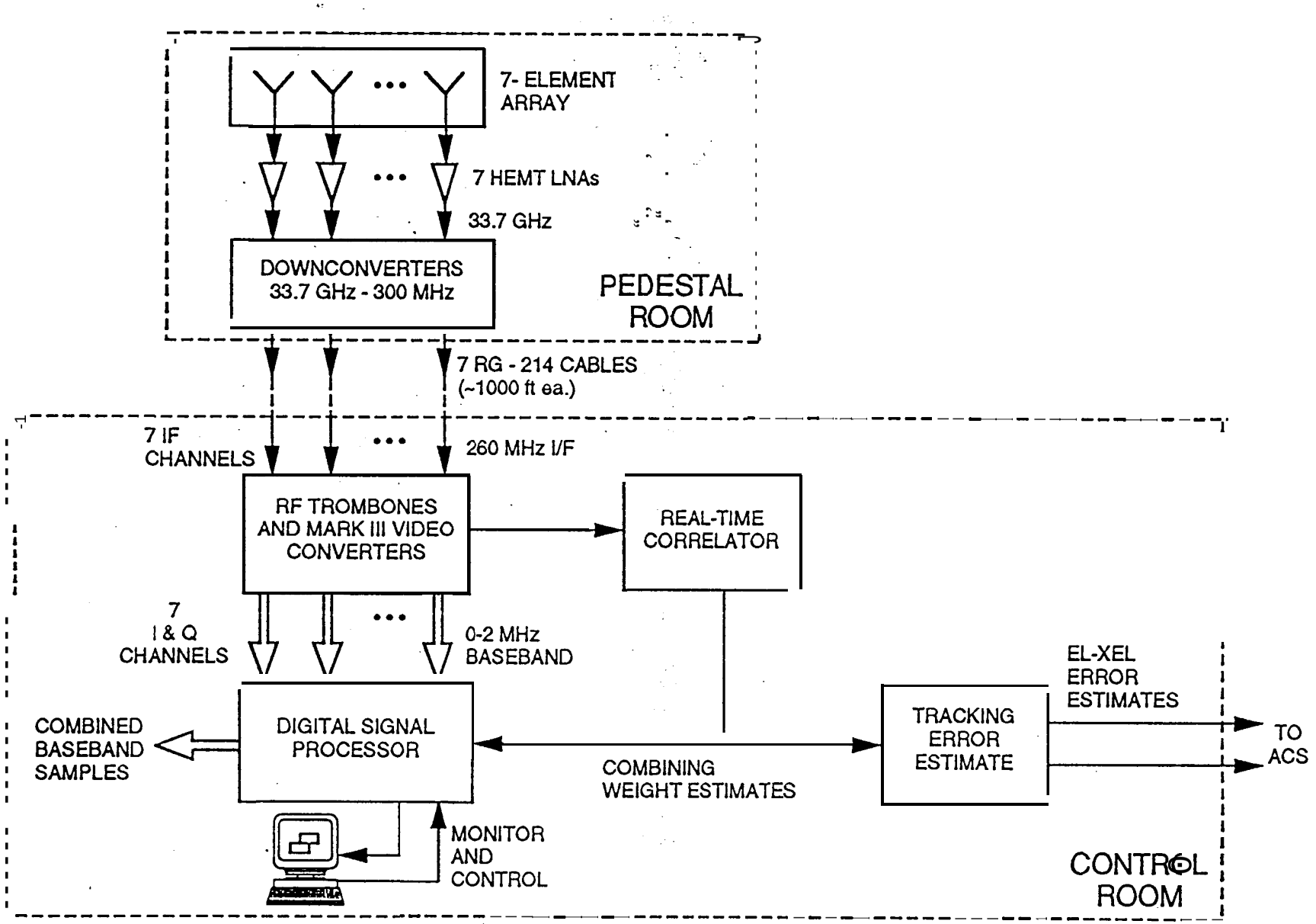

Figure 4. Array Feed Compensation System Block Diagram

6485-36450u

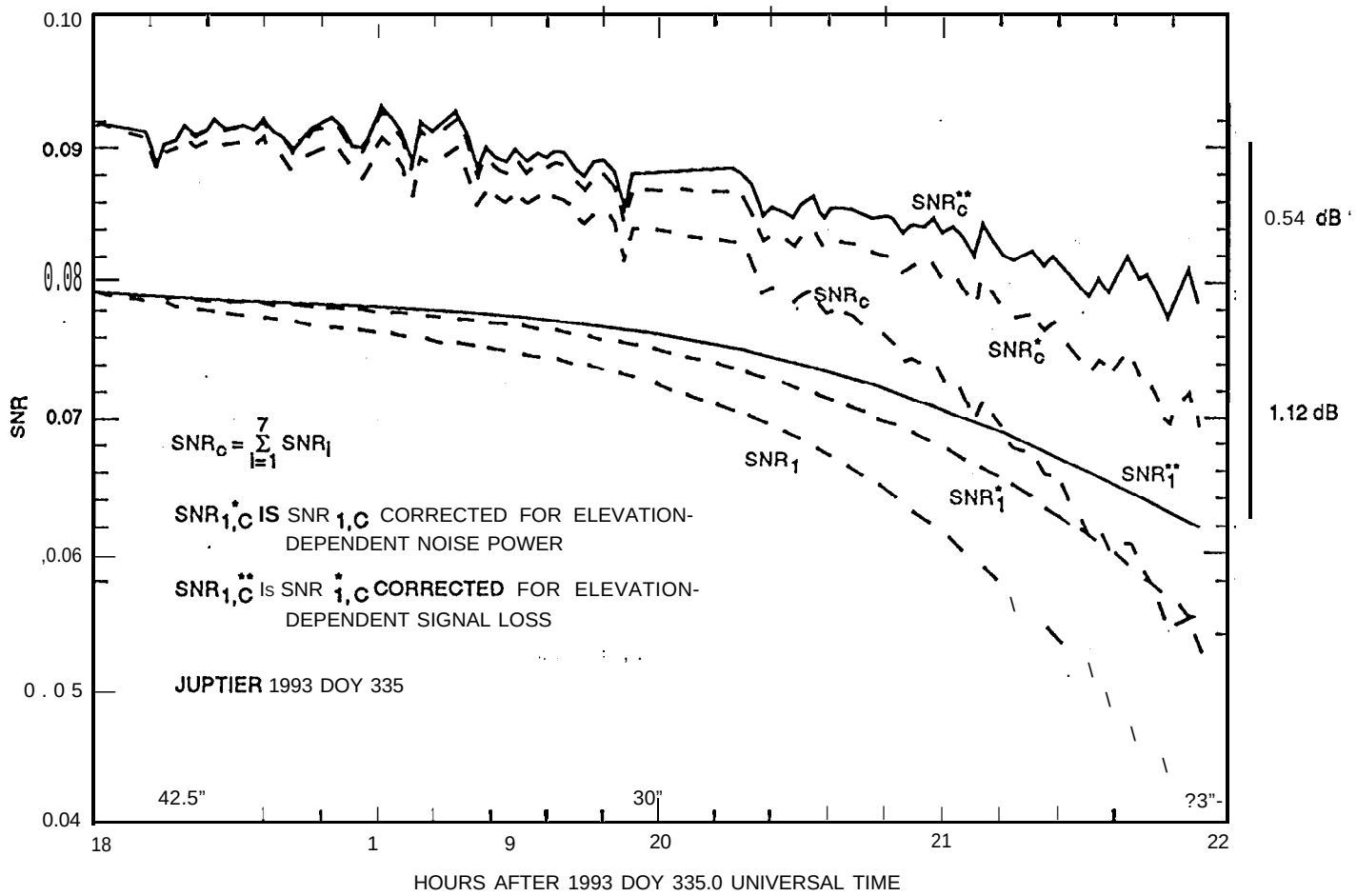

Figure 5. SNR of Combined Channel Estimated by Sum of SNR-S

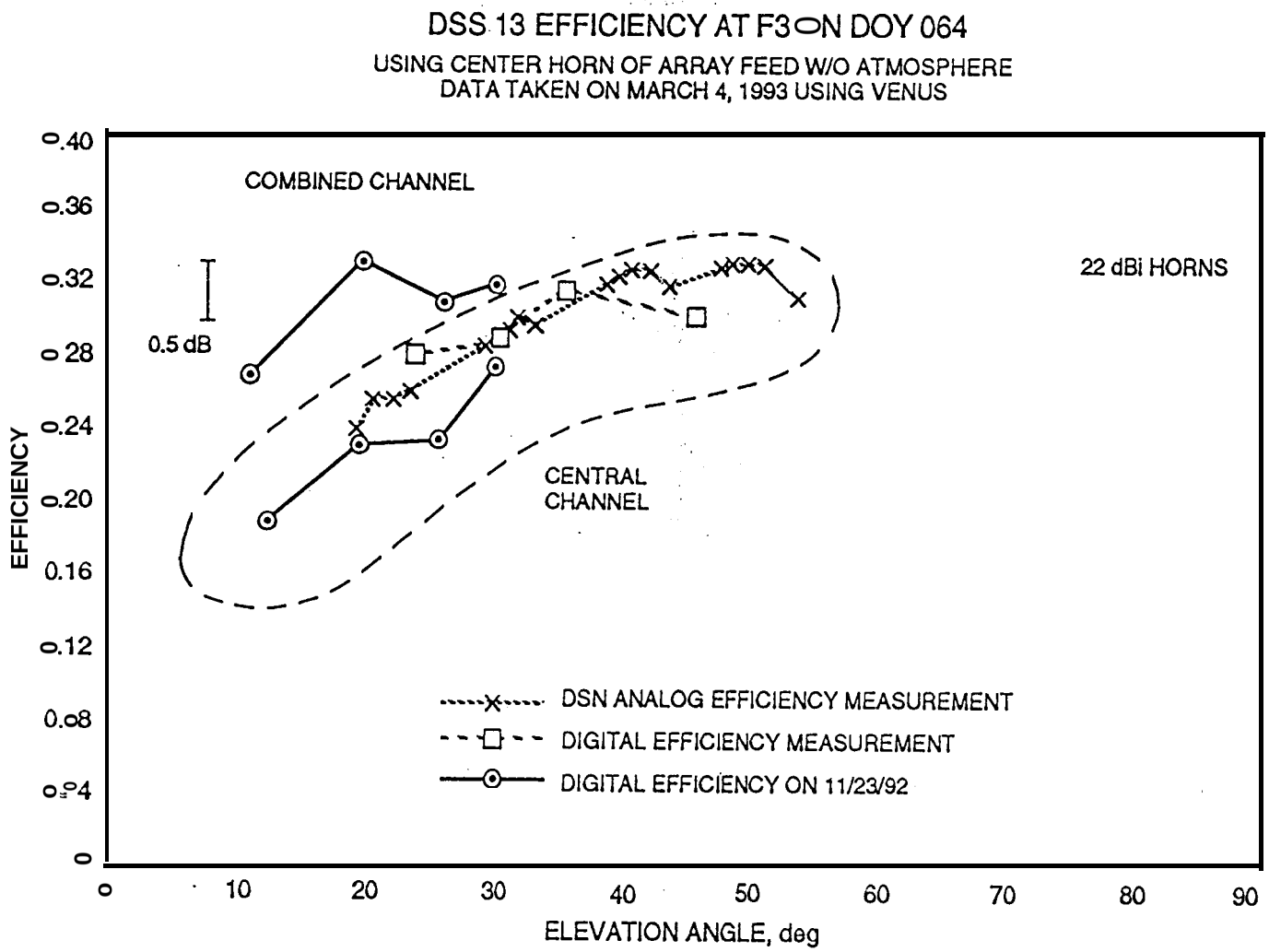

Figure 6. Preliminary Array Feed Combining System Efficiency Estimates

6485-36452u

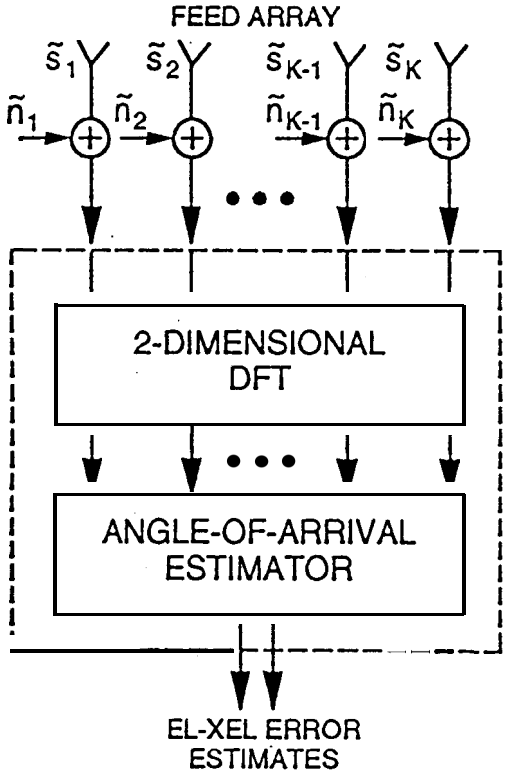

Figure 7a. Pointing Error Estimator Block Diagram

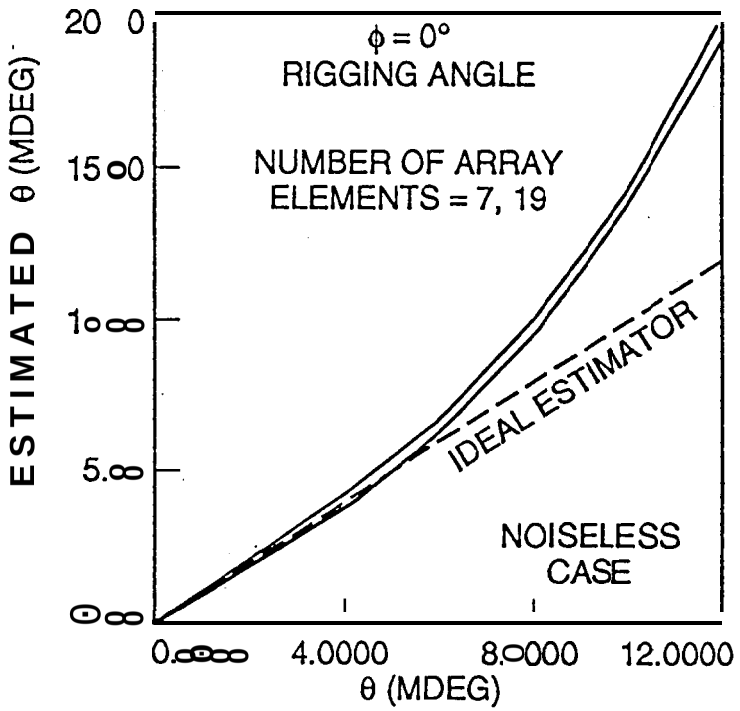

Figure 7b. Estimating Source Deviation from Boresight (θ, φ)

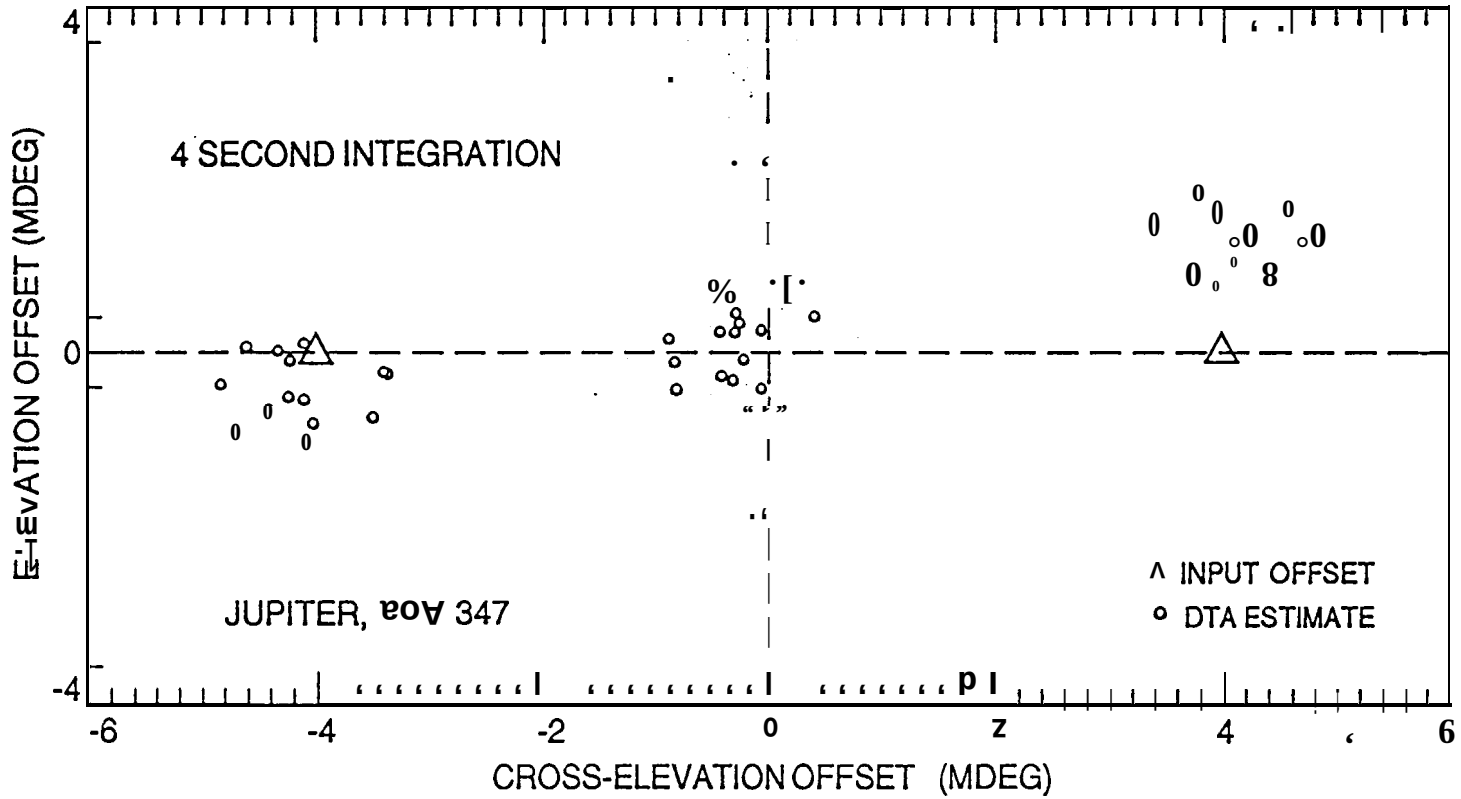

Figure 8. Tracking Algorithm Evaluation